THE JOURNAL OF BIOLOGICAL CHEMISTRY
Vol. 278, No. 7, Issue of February 14, pp. 4875–4881, 2003

Printed in U.S.A.

Hypoxic Remodeling of Ca^{2+} Stores in Type I Cortical Astrocytes*

Received for publication, September 9, 2002, and in revised form, December 2, 2002
Published, JBC Papers in Press, December 10, 2002, DOI 10.1074/jbc.M209206200

Ian F. Smith, John P. Boyle, Leigh D. Plant‡, Hugh A. Pearson‡, and Chris Peers§

From the Institute for Cardiovascular Research and the ‡School of Biomedical Sciences, University of Leeds, Leeds LS2 9JT, United Kingdom

Prolonged periods of hypoxia are deleterious to higher brain functions and increase the likelihood of developing dementias. Here, we have used fluorimetric techniques to investigate the effects of chronic hypoxia (2.5% O_2, 24 h) on Ca^{2+} stores in type I cortical astrocytes, because such stores are crucial to various astrocyte functions, including Ca^{2+}-dependent modulation of neuronal activity. Rises of $[Ca^{2+}]_i$ evoked by exposure of astrocytes to bradykinin were enhanced following chronic hypoxia, as were transient increases in $[Ca^{2+}]_i$ recorded in Ca^{2+}-free perfusate. The enhanced responses were due partly to impaired plasmalemmal Na^+/Ca^{2+} exchange following chronic hypoxia. More importantly, chronic hypoxia increased the Ca^{2+} content of mitochondria (as determined by exposing cells to mitochondrial inhibitors), such that they were unable to act as Ca^{2+} buffers following bradykinin-evoked Ca^{2+} release from the endoplasmic reticulum. Hypoxic enhancement of mitochondrial Ca^{2+} content was also observed in confocal images of cells loaded with the mitochondrial Ca^{2+} indicator, Rhod-2. Confocal imaging of cells loaded with tetramethylrhodamine ethyl ester, an indicator of mitochondrial membrane potential, indicated that mitochondria were hyperpolarized in astrocytes following chronic hypoxia. Our findings indicate that hypoxia disturbs Ca^{2+} signaling in type I astrocytes, primarily by causing mitochondrial Ca^{2+} overload.

Higher brain functions are susceptible to damage through exposure to the prolonged hypoxia of ischemia or chronic cardiorespiratory disease (1–3). Indeed, there is a well documented increased incidence of dementias in patients who have previously suffered prolonged hypoxic or ischemic episodes arising as a consequence of cardiovascular dysfunction such as stroke or arrhythmia (4–6). Such a clear link between hypoxic/ischemic episodes and increased incidence of dementias strongly suggests that lack of oxygen is a contributory factor in the precipitation of such diseases.

Many non-neuronal cell types (particularly astrocytes) contribute to intercellular signaling in the central nervous system at several levels (7–9). Astrocytes, as well as other glia, are in intimate contact with neurones and have projections that are located at neuronal synapses (10). Indeed, chemical synapses and gap junction connections between astrocytes and neurones have been identified (11, 12). Astrocytes possess receptors for numerous transmitters (*e.g.* glutamate, γ-aminobutyric acid (GABA), acetylcholine, ATP, bradykinin; reviewed in Ref. 7) and so play important, active roles in synaptic activity. Activation of astrocytes by transmitters released from neurones has been reported at levels of transmitter concentrations found outside (but adjacent to) synaptic clefts (13, 14). Astrocytic activation is usually manifest as a rise of intracellular Ca^{2+} concentration ($[Ca^{2+}]_i$) due to release of Ca^{2+} from internal stores as well as Ca^{2+} uptake from the extracellular space (9, 14–16). This fundamental initial response correlates with neuronal synaptic activity, and a rise of $[Ca^{2+}]_i$ in one astrocyte can initiate Ca^{2+} waves that propagate across significant distances via adjacent astrocytes (17–19). This represents a means of intercellular signaling in the brain that parallels and modulates classical neuronal synaptic communication and, as such, is of fundamental importance to central neuronal activity (8, 20). Within an individual astrocyte, a rise of $[Ca^{2+}]_i$ can also initiate important processes. In particular, elevated $[Ca^{2+}]_i$ triggers glutamate release which modulates neuronal activity via extrasynaptic metabotropic glutamate receptors (19, 21). Indeed, astrocytes are capable of releasing glutamate via regulated, Ca^{2+}-dependent exocytosis, in addition to reverse-mode uptake systems (17).

In the present study, we have examined how intracellular Ca^{2+} stores, key components in astrocyte Ca^{2+} signaling coupled to receptor activation via generation of inositol trisphosphate, are modulated by prolonged hypoxia. Hypoxia is a key feature of numerous cardiorespiratory diseases associated with disturbance of higher brain functions (see above), and is also a well known regulator of gene expression (22). Our results indicate that hypoxia dramatically modulates intracellular Ca^{2+} stores, primarily by causing mitochondrial Ca^{2+} loading.

MATERIALS AND METHODS

Astrocyte Culture—To obtain astrocytes, cerebral cortices were removed from 6–8 day old Wistar rat pups and placed immediately in ice-cold buffer solution consisting of 10 mM NaH_2PO_4, 2.7 mM KCl, 137 mM NaCl, 14 mM glucose, 1.5 mM $MgSO_4$, and 3 mg/ml bovine serum albumin. Meninges were removed using fine forceps, and whole cortices were then minced gently with a mechanical tissue chopper (McIlwain) and dispersed into the same buffer containing 0.25 μg/ml trypsin, at 37 °C for 15 min. Trypsin digestion was halted by the addition of an equal volume of buffer supplemented with 16 μg/ml soy bean trypsin inhibitor (SBTI, type I-S; Sigma), 0.5 μg/ml DNase I (EC 3.1.21.1 type II from bovine pancreas; 125 kilounits/ml; Sigma) and 1.5 mM $MgSO_4$. The tissue was then pelleted by centrifugation at 1300 rpm for 90 s following which the supernatant was removed and the cell pellet resuspended in 2 ml of buffer solution containing 100 μg/ml SBTI, 0.5 μg/ml DNase I, and 1.5 mM $MgSO_4$. The tissue was subsequently triturated gently with a fire polished Pasteur pipette. After allowing larger pieces of tissue to settle for 5 min, the cell suspension was taken and centrifuged at 1300 rpm for 90 s before resuspension into 60 ml of culture medium (Eagle's minimal essential medium supplemented with 10% fetal calf serum and 1% penicillin-streptomycin (GIBCO)). The cell suspension was then aliquoted into 2 × 25 cm^2 flasks and onto glass cover slips in 6- and 24-well tissue culture plates. Cells were then kept

* This work was supported by The Wellcome Trust, The Medical Research Council, and Pfizer Central Research, through a CASE studentship (to I. F. S.). The costs of publication of this article were defrayed in part by the payment of page charges. This article must therefore be hereby marked "*advertisement*" in accordance with 18 U.S.C. Section 1734 solely to indicate this fact.

§ To whom correspondence should be addressed: Inst. for Cardiovascular Research, University of Leeds, Leeds LS2 9JT, UK. Tel.: 0113-343-4174; Fax: 0113-233-4803; E-mail: c.s.peers@leeds.ac.uk.

in a humidified incubator at 37 °C (95% air; 5% CO_2). This was designated passage 1 and cells were used up to a passage of 2. 4–6 h following plating, cells were washed vigorously several times with fresh medium to remove non-adhered cells. This resulted in a culture of primarily type I cortical astrocytes (as confirmed by positive immunostaining with an anti-GFAP antibody). Culture medium was exchanged every 3–4 days, and cells were grown in culture for up to 14 days. All recordings were made from cells between days 5–12.

Cells exposed to chronic hypoxia were subcultured in the same way as control cells but 24 h prior to experimentation were transferred to a humidified incubator equilibrated with 2.5% O_2, 5% CO_2 balanced with N_2 (termed chronically hypoxic (CH)[1] conditions). Following exposure to hypoxia, cells were kept in room air for no longer than 1 h while microfluorimetric recordings took place. Corresponding control cells were maintained in a 95% air, 5% CO_2 incubator for the same period.

MTT Assay—Cell viability was assessed using the 3-(4,5-dimethylthiazol-2-yl)-2,5-diphenyltetrazolium bromide (MTT) reduction assay (23). Absorbency was measured using a spectrophotometer at a test wavelength of 570 nm and reference wavelength of 630 nm. Student's *t* test (unpaired) was used to determine the significance of differences between means, with *p* values of less than 0.05 being considered significant.

Microfluorimetric Recordings—To measure cytosolic $[Ca^{2+}]$, glass coverslips onto which cells had grown were incubated in 2 ml of control solution containing 4 μM Fura-2AM for 1 h at 21–24 °C in the dark, as previously described (24). Control solution was composed of: NaCl 135 mM, KCl 5 mM, $MgSO_4$ 1.2 mM, $CaCl_2$ 2.5 mM, Hepes 5 mM, and glucose 10 mM (pH 7.4, osmolarity adjusted to 300 mosM with sucrose, 21–24 °C). Following this incubation period, fragments of coverslips were transferred into an 80-μl recording chamber mounted on the stage of an inverted microscope, where cells were continuously perfused under gravity at a rate of 1–2 ml min^{-1}. $[Ca^{2+}]_i$ was determined using an Openlab System (Image Processing & Vision Company Ltd, Coventry, UK). Excitation was provided using a Xenon arc lamp (75 watts) and excitation wavelengths (340 and 380 nm) were selected by a monochromator (Till Photonics, Planegg, Germany). A quartz fiber-optic guide transmitted light to the microscope and was reflected by a dichroic mirror (Omega Optical, Glen Spectra Ltd, Stanmore, UK) into the objective. Emission was collected through the objective and a 510-nm filter (40-nm bandwidth). Digital images were sampled at 14-bit resolution by an intensified charge-coupled device camera (Hamamatsu Photonics, Hertfordshire, UK). Fura-2 was excited alternately at 340 and 380 nm for between 120 and 180 ms (this varied on a day-to-day basis, depending on dye-loading efficiency, but never varied between control and hypoxic cells on any given day), and ratios of the resulting images were produced every 4 s. Regions of interest (ROI) were used to restrict data collection to individual cells. All the imaging was controlled by Improvision software that included Openlab 2.2.5 (Image Processing & Vision Company Ltd, UK) and operated on a Macintosh PowerPC. Drugs and agonists were applied to cells as indicated under "Results" by switching the inflow with a 6-way Hamilton tap to one supplied by a reservoir of the relevant composition. All experiments were conducted at room temperature (21–24 °C).

For cytosolic $[Ca^{2+}]$ measurements, several parameters were determined from collected data. Changes in $[Ca^{2+}]_i$ were taken from measuring peak or plateau values and expressing them as the change in fluorescence ratio from basal levels, determined for each recording. Decay times are expressed as $t_{½}$ values *i.e.* the time taken for a response to decline to 50% of its peak value. The size of bradykinin-evoked stores was taken from the integral of transient responses recorded in Ca^{2+}-free perfusate. All results are expressed as means ± S.E., together with sample traces, and statistical comparisons were made using unpaired Student's *t*-tests. For all experiments reported, 4–8 cells in any one field of view were selected at random before the experiment was performed, and data obtained from all selected cells were included in the analysis. At least three repeats of each experiment were performed.

Mitochondrial Ca^{2+} levels were examined using a confocal system (see below), but in cells loaded with Rhod-2 (by incubation of cells with 1.5 μM Rhod-2AM for 1 h at 21 °C-24 °C in the dark, followed by a 1 h period of maintaining cells in control perfusate solution for further dye de-esterification). Rhod-2 was only excited at one wavelength (543 nm), and emission light was collected through the objective and a 570-nm filter (40-nm bandwidth). Mitochondrial membrane potential measurements were also made, using tetramethylrhodamine ethyl ester (TMRE). To load this indicator, cell monolayers incubated in 2 ml of control solution containing 300 nM TMRE for 20 min at 21 °C-24 °C in the dark. TMRE was excited at one wavelength (546 nm), and emission light was collected through the objective and a 576-nm filter (40-nm bandwidth). During TMRE fluorescence recordings, cells were continuously perfused with the same concentration of TMRE in the presence of 1 mM ascorbate (to prevent TMRE oxidation and suppress autoquenching, Ref. 25). Under these conditions photobleaching was significantly reduced, and the slow decrease in the fluorescence level caused by dye bleaching or dye loss was not considered depolarization. Changes in mitochondrial membrane potential ($\Delta\psi_m$) were determined from groups of mitochondria using the region of interest (ROI) tool. TMRE fluorescence was not calibrated to membrane potential and so is plotted as arbitrary units (256 greyscale). Confocal images were obtained from cells plated and loaded with dye as described above. Fragments of coverslips on which cells were grown were transferred to a recording chamber as described for microfluorimetric recording. This chamber was mounted on the stage of a Zeiss Axiovert 200 M inverted microscope, equipped with a C-Apochromat ×63 water immersion lens (1.2 numerical aperture) and fitted with a Zeiss LSM 510 laser-scanning module. The 543-nm laser line of a helium/neon laser was used for excitation of either Rhod-2 or TMRE-loaded cells, and the emitted light (581 nm or 574 nm respectively) collected by photomultiplier. 8 bit images (monitored using a 256 gray scale, then converted to $\Delta F/F_o$ values for comparison) were acquired as single frames (frame time 7 s), and 4 images were averaged for each frame. All experiments were performed at room temperature (21–24 °C). Loading conditions and illumination intensities and duration were kept constant for all recordings.

RESULTS

Augmentation of $[Ca^{2+}]_i$ Responses to Bradykinin Caused by Chronic Hypoxia—Fig. 1*A* shows representative, bright-field images of type I cortical astrocytes cultured under normoxic (upper) or hypoxic (lower) conditions. The cells were typically flat and elongated in appearance, and hypoxia did not noticeably alter their morphology. In order to examine cell viability under hypoxic conditions, we performed colorimetric MTT assays (23), and found that hypoxia (24–48 h) had no significant effect on cell viability as compared with cells cultured under normoxic conditions (Fig. 1*B*).

Basal Ca^{2+} levels (determined before bradykinin (BK) application) were not significantly different between chronically hypoxic (CH) and control cells, being 0.53 ± 0.03 r.u. in control cells ($n > 12$) and 0.58 ± 0.02 in CH cells ($n > 12$). When astrocytes were perfused with a solution containing 2.5 mM Ca^{2+}, bath application of 100 nM BK evoked a rapid rise of $[Ca^{2+}]_i$ due to release of Ca^{2+} from internal stores mediated by production of inositol trisphosphate, which declined with an extremely slow time course in both control and CH cells (Fig. 1*C*). This slow decline is likely due to Ca^{2+} influx (see Fig. 2, *below*). Full concentration-response relationships are presented in Fig. 1*D*, which indicates that the EC_{50} for BK was similar in both groups of cells, at ~5 nM. However, it was notable that peak BK-evoked responses were consistently greater in CH cells. Since the peak of the response reflects Ca^{2+} release from intracellular stores, rather than subsequent Ca^{2+} influx, the rest of the study employed Ca^{2+}-free perfusates (containing 1 mM EGTA) to examine release from stores in isolation, and we selected 100 nM BK as a maximally effective agonist concentration.

Chronic Hypoxia Potentiates Liberation of Ca^{2+} from Intracellular Stores by Bradykinin—In Ca^{2+}-free solution, responses to 100 nM BK were transient in both control (Fig. 2*A*, *left*) and CH (Fig. 2*A*, *right*) cells. However, a clear enhancement of responses was observed in CH cells. The bar graphs of all measured parameters are presented in Fig. 2*B*. Thus, as was the case in Ca^{2+}-containing perfusate, basal levels re-

[1] The abbreviations used are: CH, chronically hypoxic; MTT, 3-(4,5-dimethylthiazol-2-yl)-2,5-diphenyltetrazolium bromide; TMRE, tetramethylrhodamine ethyl ester; NCX, Na^+/Ca^{2+} exchanger; r.u., relative units; BK, bradykinin; CPZ, cyclopiazonic acid; ER, endoplasmic reticulum; FCCP, *p*-trifluoromethoxy carbonyl cyanide phenylhydrazone.

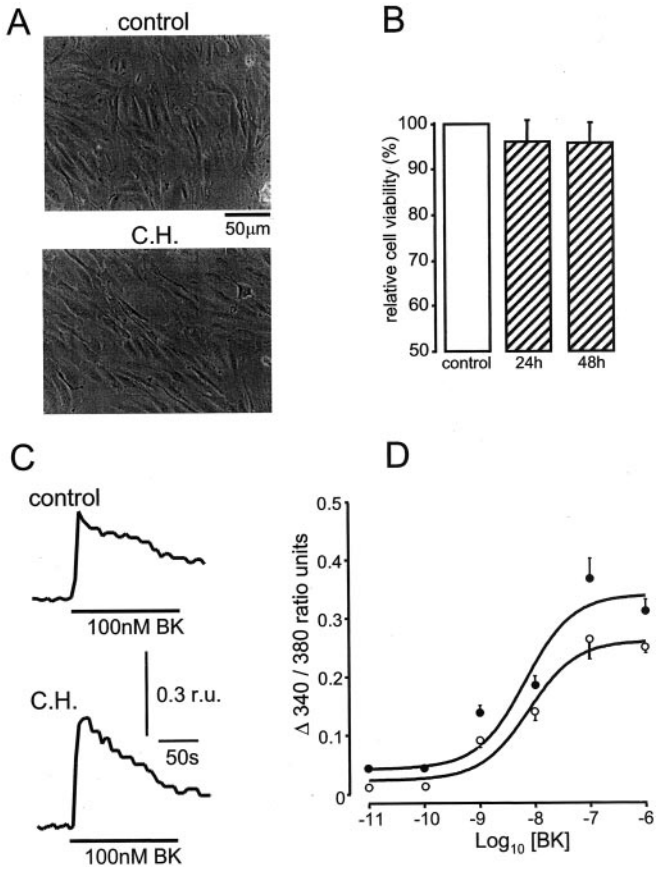

FIG. 1. **Chronic hypoxia augments $[Ca^{2+}]_i$ responses to bradykinin without affecting astrocyte viability.** *A*, bright-field phase contrast images of astrocytes used in the studies presented herein. Cells were cultured under either normoxic (*upper image*) or chronically hypoxic (*C.H.*, *lower image*) conditions. *Scale bar* applies to both images. *B*, cell viability, determined using the MTT assay, following culture under normoxic conditions (*open bar*) or chronically hypoxic conditions (*hatched bars*) for the time periods indicated. Data are normalized to control levels of cell viability. *C*, sample increases of $[Ca^{2+}]_i$ evoked by application of 100 nM BK for the period indicated by the horizontal bars in control (*upper*) and chronically hypoxic (*C.H.*, *lower*) type I cortical astrocytes. *Scale bars* apply to both traces. *D*, concentration-response relationships indicating peak rises in $[Ca^{2+}]_i$ evoked by varying concentrations of BK in control (*open circles*) and chronically hypoxic (*filled circles*) astrocytes. Each point plotted represents the mean ± S.E. response, $n = 3–6$ experiments in each case, from each of which at least three cells were measured.

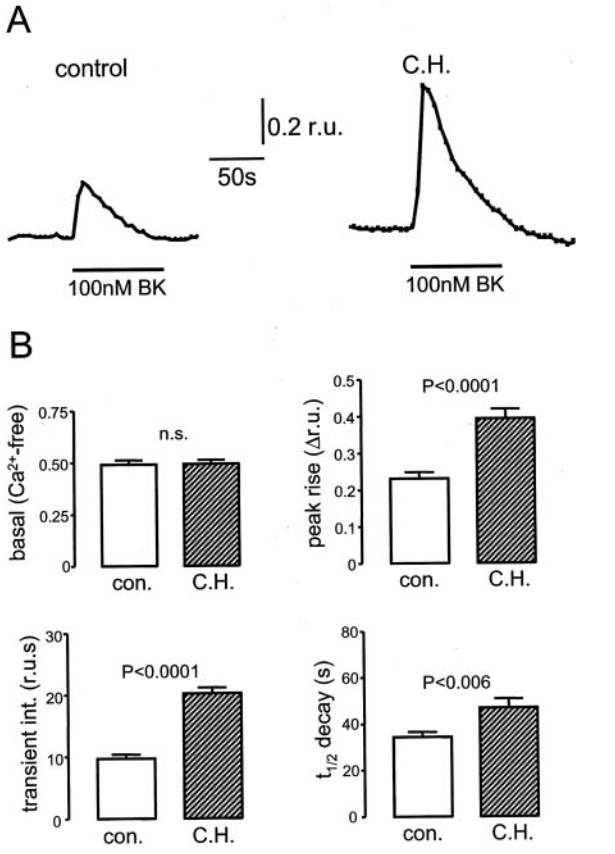

FIG. 2. **Chronic hypoxia causes apparent augmentation of Ca^{2+} liberation from intracellular stores by bradykinin.** *A*, sample rises in $[Ca^{2+}]_i$ evoked by application of 100 nM BK for the period indicated by the horizontal bars in control (*left*) and chronically hypoxic (*C.H.*, *right*) type I cortical astrocytes. For these experiments, the perfusate was nominally Ca^{2+}-free. *Scale bars* apply to both traces. *B*, bar graphs indicating mean values of parameters measured from recordings exemplified in *A*: basal $[Ca^{2+}]_i$ levels, peak responses to 100 nM BK, the integral of the transient rise of $[Ca^{2+}]_i$ evoked by BK and the time taken for the peak to decline to 50% of its maximal value. Data are means ± S.E. taken from control recordings (*open bars*) and chronically hypoxic cells (*hatched bars*). Statistical differences between control and chronically hypoxic cells are indicated by *p* values above each graph ($n = 3–6$ experiments in each case, from each of which at least four cells were measured).

corded in Ca^{2+}-free solution were not significantly different in the two cell groups. The peak rise of $[Ca^{2+}]_i$ and the total amount of Ca^{2+} liberated by BK (determined by integration of the transient response) were both significantly greater in CH cells. Finally, a significant slowing of the decay rate was also observed in CH cells, as compared with controls.

The enhancement of BK-evoked rises of $[Ca^{2+}]_i$ seen in CH cells could have been due to a more complete discharge of Ca^{2+} from internal stores in this cell group, or due to CH cells having a greater store size. To investigate this, we discharged intracellular stores completely, by exposing cells to 10 μM cyclopiazonic acid (CPZ). We found in these cells that this agent depleted stores more rapidly than the irreversible Ca^{2+}-ATPase inhibitor, thapsigargin. As illustrated in the sample traces of Fig. 3*A* and the mean data of Fig. 3*B*, the amount of Ca^{2+} discharged from intracellular stores was clearly significantly greater in CH cells than in controls. In addition, subsequent application of BK following depletion of stores with either CPZ (Fig. 3*C*) or thapsigargin (Fig. 3*D*) failed to evoke a rise in $[Ca^{2+}]_i$ in either cell group, indicating that both CPZ and thapsigargin fully discharged intracellular stores.

Chronic Hypoxia Inhibits Plasmalemmal Na^+/Ca^{2+} Exchange—While the data of Fig. 2 suggest that BK-sensitive Ca^{2+} stores are greater in CH cells, the enhanced responses could be due to altered buffering of cytosolic Ca^{2+} once liberated from stores. One such mechanism to account for the transient responses of cells to BK in Ca^{2+}-free perfusate is Ca^{2+} extrusion across the plasma membrane on transporters such as the Na^+/Ca^{2+} exchanger (NCX). To investigate the role of NCX in shaping the responses to BK, we applied the agonist in Na^+-free solutions (replaced with NMDG). As illustrated in Fig. 4*A* and the averaged data of Fig. 4*B*, this maneuver caused a small increase in the peak $[Ca^{2+}]_i$ response, which did not reach statistical significance. However, there was a significant increase in the transient integral, due to a slowing of the time course of decay (Fig. 4*B*). In CH cells, no significant differences were observed in either the amplitude or time course of the response (Fig. 4, *A* and *B*). These results indicate that NCX is not the major mechanism for Ca^{2+} extrusion following release from intracellular stores in astrocytes, and also that modulation of such exchange cannot account for the enhanced responses observed in CH cells. However, perhaps more importantly, the significant influence of NCX in shaping the

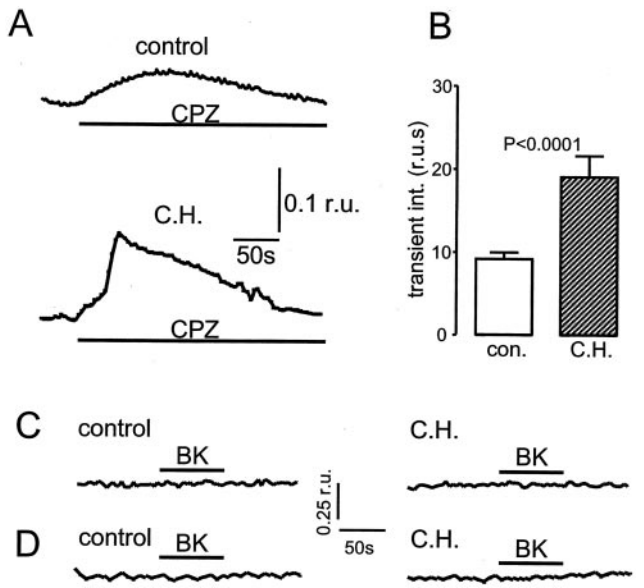

FIG. 3. **Cyclopiazonic acid and thapsigargin fully deplete BK-sensitive intracellular Ca^{2+} stores in astrocytes.** *A*, representative rises in $[Ca^{2+}]_i$ evoked by bath application of cyclopiazonic acid (CPZ; 10 μM which was present for the period indicated by the *horizontal bar*) in control (*upper trace*) and chronically hypoxic (*C.H.*; *lower trace*) astrocytes. *Scale bars* apply to both traces. *B*, *bar graph* indicating mean integrals (with S.E. bars) of the transient rise of $[Ca^{2+}]_i$ evoked by CPZ. Data are taken from control recordings (*open bars*) and chronically hypoxic cells (*hatched bars*). Statistical difference between control and C.H. cells is indicated by p value shown ($n = 4-6$ experiments in each case, from each of which at least four cells were measured). *C*, sample lack of response to BK in control (*left*) and chronically hypoxic (*right*) astrocytes following 5-min pretreatment with 10 μM CPZ. *D*, as in *C*, except that cells were previously exposed to 1 μM thapsigargin for 20 min prior to recording. *Scale bars* apply to *C* and *D*.

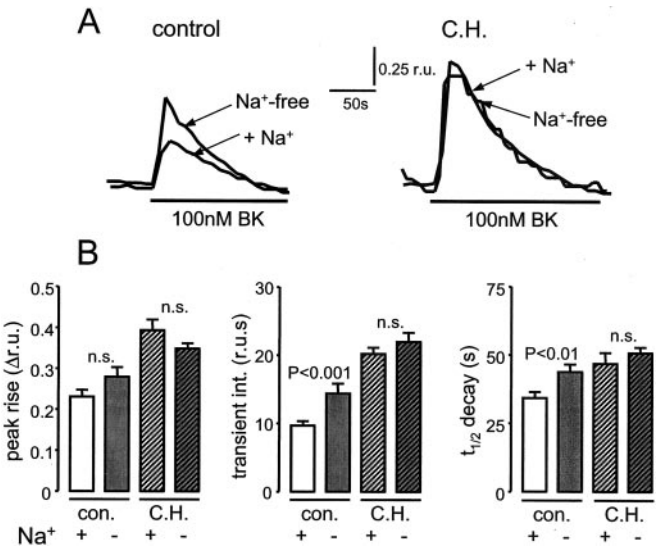

FIG. 4. **Chronic hypoxia inhibits plasmalemmal Na^+/Ca^{2+} exchange.** *A*, sample rises in $[Ca^{2+}]_i$ evoked by application of 100 nM BK for the period indicated by the horizontal bars in control (*left*) and chronically hypoxic (*C.H.*, *right*) type I cortical astrocytes. In each case, the perfusate was Ca^{2+}-free and either contained Na^+, or Na^+ was replaced with NMDG (Na^+-free, as indicated). *Scale bars* apply to both traces. *B*, *bar graphs* indicating mean values of parameters measured from recordings exemplified in *A*: peak responses to 100 nM BK, the integral of the transient rise of $[Ca^{2+}]_i$ evoked by BK and the time taken for the peak to decline to 50% of its maximal value. Data are means ± S.E. taken from six control recordings in the presence of Na^+ (*open bars*) or in its absence (*shaded bars*) and nine chronically hypoxic cells in the presence of Na^+ (*hatched bars*) or in its absence (*hatched*, *shaded bars*), as indicated. Statistical differences between control and chronically hypoxic cells are indicated by p values above each graph. ($n = 4-6$ experiments in each case, from each of which at least four cells were measured).

responses seen in control cells was not present in CH cells.

Chronic Hypoxia Potentiates Mitochondrial Ca^{2+} Loading—Recent studies have indicated that inhibition of NCX can arise due to excessive Ca^{2+} loading of mitochondria (26). We therefore explored the possible involvement of mitochondria in the enhancement of BK-evoked rises in $[Ca^{2+}]_i$. Fig. 5*A* (*left*) illustrates a recording from a control cell, which was firstly exposed to the mitochondrial inhibitor FCCP (10 μM), which was applied together with 2.5 μg/ml oligomycin (to prevent ATP consumption by the F_1F_0-ATP synthase functioning in reverse mode). This caused a transient rise of cytosolic $[Ca^{2+}]$. In the continued presence of FCCP and oligomycin, application of 100 nM BK evoked rises in control cells that were significantly greater than those evoked without mitochondrial inhibition (Fig. 2). Responses in CH cells (*e.g.* Fig. 5*A*, *right*) differed from those seen in control cells in two important aspects. Firstly, mitochondrial inhibition caused significantly greater rises of $[Ca^{2+}]_i$ (mean data shown in Fig. 5*B*) and secondly, the subsequent application of BK evoked rises in $[Ca^{2+}]_i$, which were not significantly different from those observed in CH cells in the absence of mitochondrial inhibitors. It is also noteworthy that during mitochondrial inhibition, there were no significant differences in the responses to BK observed between control and CH cells, as determined by integration of the transients.

Data presented in Fig. 5 suggest that the cytosolic Ca^{2+} response to BK may be attenuated in control (but not CH) cells due to Ca^{2+} uptake by mitochondria. In further support of this idea, responses to 10 μM CPZ were also significantly potentiated (from 9.15 ± 0.84 r.u. ($n = 14$) to 19.1 ± 2.56 r.u., $p < 0.002$, $n = 18$) during mitochondrial inhibition with FCCP (10 μM) and oligomycin (2.5 μg/ml), as Fig. 6 illustrates.

The enhanced response to FCCP and oligomycin observed in CH cells (Fig. 5*A*, *right*) strongly suggested that CH caused excessive mitochondrial Ca^{2+} accumulation, as compared with controls. To investigate this in more detail, we examined confocal images of control and CH cells loaded with the mitochondrial Ca^{2+} indicator, Rhod-2. To visualize the structure of mitochondria in these cells, we firstly labeled mitochondria with Mitotracker (Fig. 7*A*). Clearly, mitochondria form extensive, complex networks in both control and chronically hypoxic cells, and the mitochondrial density did not appear altered by chronic hypoxia. Fig. 7*B* shows typical images taken under identically matched exposure conditions in control and CH astrocytes, at two levels of magnification. Mitochondria are evident from their distribution and shape throughout the cell (see for example Ref. 27), although the Rhod-2 images appear more fragmented that the images obtained with Mitotracker. Clearly, fluorescence is greater in the CH cells. The dashed lines in each upper trace show the point at which a line scan was performed, and the corresponding pixel intensities are plotted in Fig. 7*C*. Peaks in each trace correspond to the line scan crossing mitochondria, and such peaks are consistently greater in CH cells, reflecting a higher mitochondrial Ca^{2+} content. It is noteworthy that while the peaks in the line scans were greater in amplitude in CH astrocytes, the absolute number was similar, indicating that hypoxia did not increase the number or density of mitochondria. These traces were typical of at least six different images of both control and CH astrocytes. While not quantitative, these data further support the Fura-2 data of Fig. 5 indicating that CH causes increased mitochondrial Ca^{2+} loading.

Chronic Hypoxia Hyperpolarizes Mitochondrial Membrane Potential—Accumulation of Ca^{2+} by mitochondria is dependent on the maintenance of the mitochondrial membrane potential,

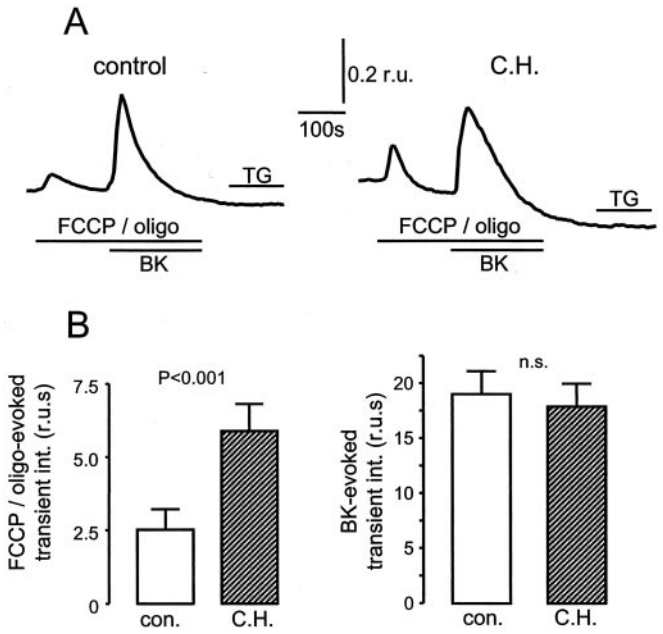

FIG. 5. **Chronic hypoxia enhances mitochondrial Ca^{2+} content.** *A*, sample rises in $[Ca^{2+}]_i$ evoked by application of 10 μM FCCP together with 2.5 μg/ml oligomycin, and in the additional presence of 100 nM BK. Following washout, cells were exposed to 1 μM thapsigargin (*TG*). Drug applications were for the periods indicated by the horizontal bars in control (*left*) and chronically hypoxic (*C.H.*, *right*) astrocytes. In each case, the perfusate was Ca^{2+}-free, and *scale bars* apply to both traces. *B*, *bar graph* indicating mean integrals (with S.E. bars) of the transient rise of $[Ca^{2+}]_i$ evoked by FCCP and oligomycin (*left*), and by BK in the continued presence of FCCP and oligomycin (*right*). Data are taken from control recordings (*open bars*) and chronically hypoxic cells (*hatched bars*). Statistical difference between control and C.H. cells is indicated by *p* value shown. (n = 4–6 experiments in each case, from each of which at least three cells were measured).

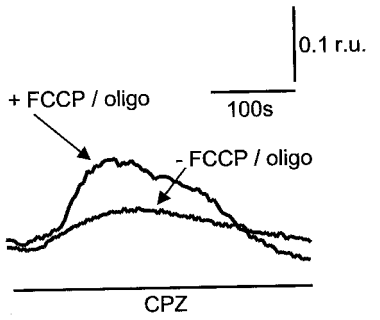

FIG. 6. **Mitochondrial inhibition enhances CPZ-evoked Ca^{2+} transients.** Representative rises in $[Ca^{2+}]_i$ evoked by bath application of cyclopiazonic acid (CPZ; 10 μM which was present for the period indicated by the *horizontal bar*) in untreated controls (taken from Fig. 3 for clarity) and in control cells during continued exposure to 10 μM FCCP and 2.5 μg/ml oligomycin (which were applied 1 min before the commencement of the traces), as indicated.

(Ψ_m). We therefore examined whether Ψ_m differed between control and CH cells, using the Ψ_m indicator, TMRE. As can be seen from Fig. 8*A*, confocal images were consistently brighter in CH cells as compared with control cells. While individual mitochondria could not be resolved with the clarity found using Rhod-2 (Fig. 7), staining appeared more punctate in CH cells, consistent with greater accumulation into specific organelles. Furthermore, the regions of brightest intensity (in both control and CH cells) were found in parts of cells close to nuclei. This is also reflected in the line scan plots of Fig. 8*B* (made using lines indicated in the corresponding images), where in each case peaks are seen either side of a trough in the plot which represents scanning over the nuclear region of the image.

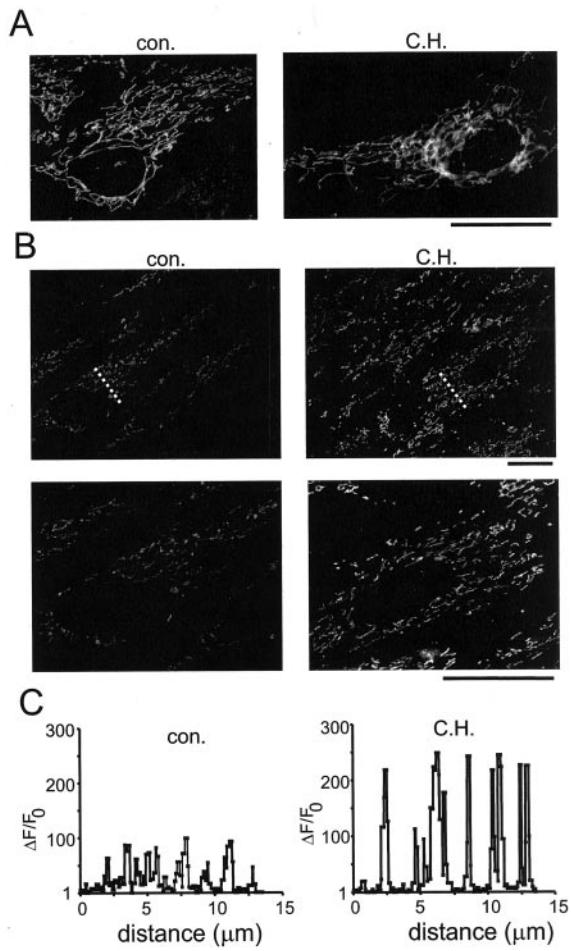

FIG. 7. **Chronic hypoxia increases the Ca^{2+} content of mitochondria in astrocytes.** *A*, confocal images of control (*left*) and CH (*right*) astrocytes stained with the mitochondrial marker, Mitotracker. *B*, *upper traces*, confocal images of control (*left*) and CH (*right*) astrocytes loaded with the mitochondrial Ca^{2+} indicator, Rhod-2. The *dashed line* in each case shows the line of scan used to generate the plots in *C*, and in each case is 14 μm in length. *Lower traces,* higher resolution images acquired as for *upper traces*. *Scale bars* shown at the *bottom left* of each pair of images in *A* and *B* indicate 15 μm. *C*, plots of pixel intensity along the lines of scan shown in *B* (*upper traces*). Peaks in each trace correspond to line scan crossing individual mitochondria.

These peaks are clearly greater in the CH cells, an observation consistently seen in at least six separate experiments.

We also employed TMRE to monitor fluorescent signals using conventional (non-confocal) imaging, while cells were under continual perfusion. Again, fluorescence observed in CH cells was clearly greater than in control cells, and the brightest regions of each cell were found in cytosolic areas close to the nucleus (Fig. 9*A*). Despite continual loss of signal, we could also observe an increased rate of signal loss in both cell types when exposed to 10 μM FCCP in the presence of 2.5 μg/ml oligomycin (Fig. 9*A*, *lower traces*, and Fig. 9*B*). These findings strongly suggest that CH causes a hyperpolarization of $\Delta\Psi_m$, an effect which is most likely responsible for the increased mitochondrial accumulation of Ca^{2+} indicated by experiments described earlier.

DISCUSSION

Cellular effects of cerebral hypoxia/ischemia have received intense interest over many years, not only because of the associated neuronal damage and death (28, 29), but also because prolonged, milder hypoxic episodes can lead to deleterious effects on higher brain functions (1–3) and also to an increased likelihood of subsequent development of dementias (4–6). The

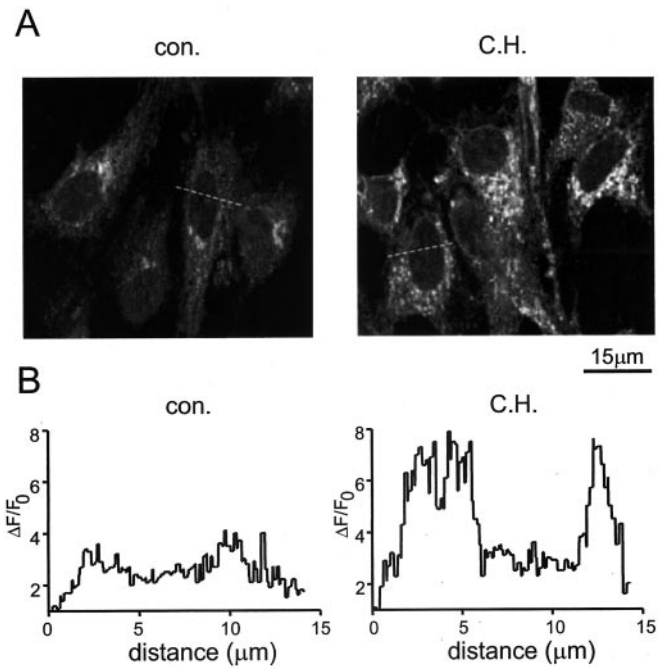

FIG. 8. **Chronic hypoxia hyperpolarizes astrocyte mitochondrial membrane potential.** *A*, confocal images of control (*left*) and CH (*right*) astrocytes loaded with the Ψ_m indicator, TMRE. The *dashed line* in each case shows the line of scan used to generate the plots in *B*, and in each case is 14 μm in length. *B*, plots of pixel intensity along the lines of scan shown in *A*.

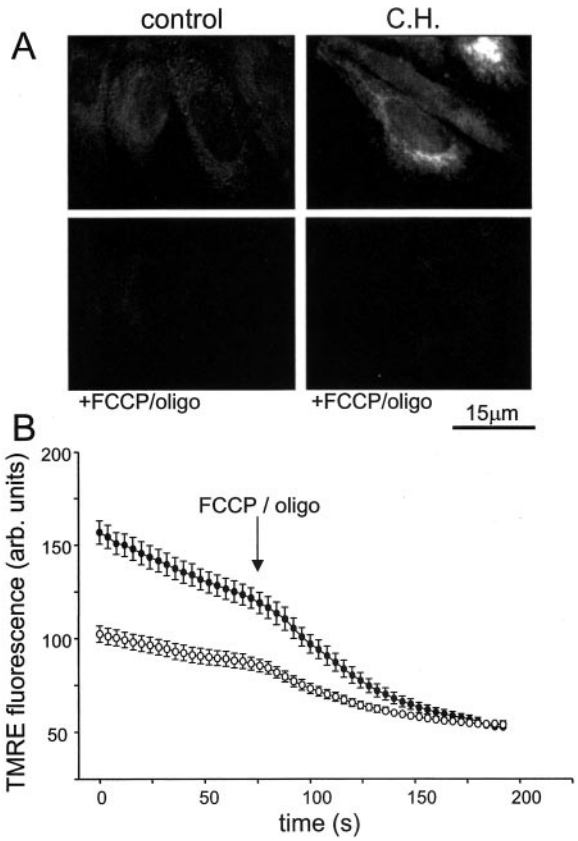

FIG. 9. **Dissipation of mitochondrial membrane potential by FCCP.** *A*, fluorescent images obtained from control (*left*) and chronically hypoxic (*C.H.*, *right*) astrocytes. Images were obtained before (*upper*) and after (*lower*) bath application of 10 μM FCCP and 2.5 μg/ml oligomycin. *Calibration bar* applies to all images. *B*, mean time course of the decline in TMRE fluorescence in control (*open circles*, $n = 12$ cells) and chronically hypoxic (*filled circles*, $n = 14$ cells). At the point indicated by the *arrow*, the Ca^{2+}-free perfusate was exchanged for one containing 10 μM FCCP and 2.5 μg/ml oligomycin.

majority of studies to date have focused on the effects of hypoxia/ischemia on central neurones, with perhaps less attention given to astrocytes or other, non-neuronal cell types in the central nervous system. The importance of astrocyte function to central intercellular signaling is currently receiving increasing attention (see the Introduction), in part due to emerging awareness of their anatomical proximity and important physiological regulation of neuronal synaptic transmission (11–14).

Since Ca^{2+} signaling is one of the major forms of communication between astrocytes and is also a major factor in the physiological activity of individual astrocytes, we have addressed the question of whether prolonged hypoxia can modulate such signaling, using primary cultures of rat type I cortical astrocytes, a well established system for studying astrocyte function, and their robust responses to BK (30–32). Our initial observation was that BK evoked significantly greater release of Ca^{2+} from intracellular stores in CH cells than was observed in control cells (Fig. 2). This was not due to altered intracellular signaling between BK receptors and Ca^{2+} stores, since CPZ also liberated more Ca^{2+} from stores in CH cells (Fig. 3). Likely possibilities to account for this were that the BK-sensitive (endoplasmic reticulum; ER) stores contained greater levels of Ca^{2+} following chronic hypoxia or that, once liberated from the ER, Ca^{2+} was less efficiently cleared and so could accumulate in the cytosol to a greater concentration. Mechanisms for cytosolic Ca^{2+} clearance include re-uptake into ER stores or other organelles, and Ca^{2+} extrusion via NCX or Ca^{2+}-ATPase. Reuptake into the ER was deemed unlikely in the continued presence of agonist, and so we firstly investigated a possible role of NCX. This was also prompted by a recent report indicating that ongoing, acute hypoxia inhibits NCX in vascular smooth muscle (33). Results presented in Fig. 4 indicate that in control cells, NCX plays a significant role in shaping the transient rise of cytosolic $[Ca^{2+}]$ when ER stores are discharged with BK. By contrast, NCX appeared to be non-functional in CH cells (Fig. 4). Thus, CH somehow appeared to inhibit NCX in cortical astrocytes. Importantly, however, the absence of functional NCX could not account fully for the enhanced cytosolic rise in $[Ca^{2+}]$ seen in response to BK application in CH cells.

At present, the underlying mechanisms accounting for inhibition of NCX by prolonged hypoxia remain to be determined. However, a recent report has demonstrated that accumulation of Ca^{2+} by mitochondria specifically inhibits NCX in COS cells transfected with a bovine Na^+/Ca^{2+} exchanger (26). On the basis of this report, we investigated the Ca^{2+} content of mitochondria in astrocytes. Fig. 5 clearly demonstrates that CH leads to excessive Ca^{2+} loading of mitochondria, as evidenced by the enhanced response to application of FCCP and oligomycin, and this observation is reinforced by the confocal images of astrocytes loaded with the mitochondrial Ca^{2+} indicator, Rhod-2 (Fig. 7). Additionally, the subsequent exposure to BK (and also to CPZ; Fig. 6) in the continued presence of mitochondrial inhibitors caused a markedly increased rise of cytosolic $[Ca^{2+}]$ in control cells, while responses in CH cells were unchanged. These data indicate that, in control astrocytes, BK-evoked rises in $[Ca^{2+}]_i$ are limited due to Ca^{2+} buffering into mitochondria. This finding is in accordance with numerous studies, which have documented the close anatomical and functional interactions of mitochondria and the ER (*e.g.* Refs. 34–36). Importantly, Ca^{2+} buffering into mitochondria does not appear to occur in CH cells, presumably because the mitochondria in these cells already contain excessive amounts of Ca^{2+} and so are incapable of acquiring more. Such a suggestion is

supported strongly by the Rhod-2 confocal images and associated pixel intensity lines scans of Fig. 7, which demonstrated marked increases in punctate staining in CH cells. Such mitochondrial accumulation of Ca^{2+} is most likely due to mitochondrial hyperpolarization (upon which mitochondrial Ca^{2+} accumulation is dependent), a view supported by both confocal and conventional images acquired using the indicator TMRE. This dye accumulates in mitochondria in proportion to the Ψ_m; the more hyperpolarized Ψ_m is, the more dye accumulates. Clearly, in CH cells, increased (and more punctate) fluorescence was observed which reflects a hyperpolarization of mitochondria in astrocytes following a period of prolonged hypoxia.

Thus, the present study indicates that CH causes mitochondrial hyperpolarization, which is likely to account for excessive accumulation of Ca^{2+}, although a possible additional effect of hypoxia to inhibit mitochondrial Na^+/Ca^{2+} exchange has not been discounted, and is worthy of future study. Two important consequences arise from this mitochondrial Ca^{2+} overload: firstly, via a mechanism yet to be identified, mitochondrial Ca^{2+} loading inhibits the plasmalemmal NCX (see also Ref. 26). Secondly, Ca^{2+}-overloaded mitochondria are unable to participate in buffering of Ca^{2+} liberated into the cytosol from the ER following agonist application. The mechanism(s) by which prolonged hypoxia leads to hyperpolarization of Ψ_m will be the focus of future work. A recent study has suggested that Ψ_m can be hyperpolarized by Ca^{2+}-dependent dephosphorylation of cytochrome *c* oxidase (37). This "molecular-physiological hypothesis" (see also Ref. 38) is dependent on the mitochondrial ATP: ADP ratio, which may well be altered under hypoxic conditions. Importantly, this hyperpolarization in turn leads to increased formation of reactive oxygen species (ROS), and ROS have been suggested by others to cause irreversible inhibition of the plasmalemmal Na^+/Ca^{2+} exchanger (39), a suggestion consistent with our observed lack of NCX function seen in CH astrocytes (Fig. 4).

The concept that cellular ROS levels increase during prolonged periods of hypoxia is not uncontested, but is currently gathering momentum. Recently, a number of groups have suggested that the source of increased cellular ROS during hypoxia is mitochondrial (37, 38, 40–43). The present study is also in accordance with these findings, and indicates that hypoxia may increase ROS production via mitochondrial hyperpolarization. Our findings are likely to have important implications for the understanding of cellular damage and death in the central nervous system following periods of hypoxia or ischemia (44, 45).

REFERENCES

1. Incalzi, R. A., Gemma, A., Marra, C., Muzzolon, R., Capparella, O., and Carbonin, P. (1993) *Am. Rev. Respir. Dis.* **148,** 418–424
2. Kogure, K., and Kato, H. (1993) *Stroke* **24,** 2121–2127
3. Koistinaho, J., Pyykonen, I., Keinanen, R., and Hokfelt, T. (1996) *Neuroreport* **7,** 2727–2731
4. Tatemichi, T. K., Paik, M., Bagiella, E., Desmond, D. W., Stern, Y., Sano, M., Hauser, W. A., and Mayeux, R. (1994) *Neurology* **44,** 1885–1891
5. Kokmen, E., Whisnant, J. P., O'Fallon, W. M., Chu, C. P., and Beard, C. M. (1996) *Neurology* **46,** 154–159
6. Moroney, J. T., Bagiella, E., Desmond, D. W., Paik, M. C., Stern, Y., and Tatemichi, T. K. (1996) *Stroke* **27,** 1283–1289
7. Verkhratsky, A., Orkand, R. K., and Kettenmann, H. (1998) *Physiol. Rev.* **78,** 99–141
8. Bezzi, P., and Volterra, A. (2001) *Curr. Opin. Neurobiol.* **11,** 387–394
9. Bezzi, P., Domercq, M., Vesce, S., and Volterra, A. (2001) *Prog. Brain Res.* **132,** 255–265
10. Ventura, R., and Harris, K. M. (1999) *J. Neurosci.* **19,** 6897–6906
11. Bergles, D. E., Roberts, J. D., Somogyi, P., and Jahr, C. E. (2000) *Nature* **405,** 187–191
12. Alvarez-Maubecin, V., Garcia-Hernandez, F., Williams, J. T., and Van Bockstaele, E. J. (2000) *J. Neurosci.* **20,** 4091–4098
13. Parpura, V., Basarsky, T. A., Liu, F., Jeftinija, K., Jeftinija, S., and Haydon, P. G. (1994) *Nature* **369,** 744–747
14. Kang, J., Jiang, L., Goldman, S. A., and Nedergaard, M. (1998) *Nat. Neurosci.* **1,** 683–692
15. Grosche, J., Matyash, V., Moller, T., Verkhratsky, A., Reichenbach, A., and Kettenmann, H. (1999) *Nat. Neurosci.* **2,** 139–143
16. Deitmer, J. W., Verkhratsky, A. J., and Lohr, C. (1998) *Cell Calcium* **24,** 405–416
17. Araque, A., Carmignoto, G., and Haydon, P. G. (2001) *Annu. Rev. Physiol.* **63,** 795–813
18. Giaume, C., and Venance, L. (1998) *Glia* **24,** 50–64
19. Pasti, L., Zonta, M., Pozzan, T., Vicini, S., and Carmignoto, G. (2001) *J. Neurosci.* **21,** 477–484
20. Fam, S. R., Gallagher, C. J., and Salter, M. W. (2000) *J. Neurosci.* **20,** 2800–2808
21. Carmignoto, G. (2000) *Prog. Neurobiol.* **62,** 561–581
22. Beitner-Johnson, D., Shull, G. E., Dedman, J. R., and Millhorn, D. E. (1997) *Respir. Physiol.* **110,** 87–97
23. Mosmann, T. (1983) *J. Immunol. Methods* **65,** 55–63
24. Smith, I. F., Boyle, J. P., Vaughan, P. F., Pearson, H. A., and Peers, C. (2001) *J. Neurochem.* **79,** 877–884
25. Tsien, R. Y., and Waggoner, A. (1994) in *Handbook of Confocal Microscopy* (Pawley, J., ed), pp. 267–280, Plenum Press, New York
26. Opuni, K., and Reeves, J. P. (2000) *J. Biol. Chem.* **275,** 21549–21554
27. Collins, T. J., Berridge, M. J., Lipp, P., and Bootman, M. D. (2002) *EMBO J.* **21,** 1616–1627
28. Choi, D. W. (1990) *J. Neurosci.* **10,** 2493–2501
29. Choi, D. W. (1995) *Trends Neurosci.* **18,** 58–60
30. Stephens, G. J., Cholewinski, A. J., Wilkin, G. P., and Djamgoz, M. B. (1993) *Glia* **9,** 269–279
31. Gimpl, G., Walz, W., Ohlemeyer, C., and Kettenmann, H. (1992) *Neurosci. Lett.* **144,** 139–142
32. Sergeeva, M., Ubl, J. J., and Reiser, G. (2000) *Neuroscience* **97,** 765–769
33. Wang, Y. X., Dhulipala, P. K., and Kotlikoff, M. I. (2000) *FASEB J.* **14,** 1731–1740
34. Barrett, E. F. (2001) *J. Gen. Physiol* **118,** 79–82
35. Landolfi, B., Curci, S., Debellis, L., Pozzan, T., and Hofer, A. M. (1998) *J. Cell Biol.* **142,** 1235–1243
36. Rutter, G. A., and Rizzuto, R. (2000) *Trends Biochem. Sci.* **25,** 215–221
37. Lee, I., Bender, E., and Kadenbach, B. (2002) *Mol. Cell Biochem.* **234–235,** 63–70
38. Lee, I., Bender, E., Arnold, S., and Kadenbach, B. (2001) *Biol. Chem.* **382,** 1629–1636
39. Nicholls, D. G., and Ward, M. W. (2000) *Trends Neurosci.* **23,** 166–174
40. Chandel, N. S., and Schumacker, P. T. (2000) *J. Appl. Physiol.* **88,** 1880–1889
41. Waypa, G. B., Chandel, N. S., and Schumacker, P. T. (2001) *Circ. Res.* **88,** 1259–1266
42. Chandel, N. S., Maltepe, E., Goldwasser, E., Mathieu, C. E., Simon, M. C., and Schumacker, P. T. (1998) *Proc. Natl. Acac. Sci. U. S. A.* **95,** 11715–11720
43. Hohler, B., Lange, B., Holzapfel, B., Goldenberg, A., Hanze, J., Sell, A., Testan, H., Moller, W., and Kummer, W. (1999) *FEBS Lett.* **457,** 53–56
44. Nicholls, D. G., and Budd, S. L. (2000) *Physiol. Rev.* **80,** 315–360
45. Budd, S. L. (1998) *Pharmacol. Ther.* **80,** 203–229